ACS Catalysis

RESEARCH ARTICLE

pubs.acs.org/acscatalysis

Catalytic Activity of Faceted Gold Nanoparticles Studied by a Model Reaction: Evidence for Substrate-Induced Surface Restructuring

Stefanie Wunder,[†] Yan Lu,[†] Martin Albrecht,[‡] and Matthias Ballauff*[,†]

[†]Soft Matter and Functional Materials, Helmholtz-Zentrum Berlin für Materialien und Energie, Hahn-Meitner-Platz 1, 14109 Berlin, Germany and Institute of Physics, Humboldt-University Berlin, Germany

[‡]Leibniz-Institut für Kristallzüchtung (IKZ), Max-Born-Strasse 2, 12489 Berlin, Germany

Supporting Information

ABSTRACT: We present the analysis of the catalytic activity of gold nanoparticles in aqueous solution as a function of temperature. As a model reaction, the reduction of *p*-nitrophenol (Nip) by sodium borohydride (BH_4^-) is used. The gold nanoparticles are immobilized on cationic spherical polyelectrolyte brushes that ensure their stability against aggregation. High-resolution transmission electron microscopy shows that the Au nanoparticles are faceted nanocrystals. The average size of the nanoparticles is 2.2 nm, and the total surface area of all nanoparticles could be determined precisely and was used in the subsequent kinetic analysis. Kinetic data have been obtained between 10 and 30 °C by monitoring the concentrations of Nip and BH_4^- by UV−vis spectroscopy. The reaction starts after an induction time t_0, and the subsequent stationary phase yields the apparent reaction rate, k_{app}. All kinetic data could be modeled in terms of the Langmuir−Hinshelwood model; that is, both reactants must be adsorbed onto the surface to react. The analysis of the temperature dependence of k_{app} leads to the heat of adsorption of both Nip and BH_4^- and the surface of the Au nanoparticles. Moreover, the true activation energy of the surface reaction is obtained. The analysis of t_0 reveals clearly that the induction period is not related to the limitations due to diffusion but to the surface restructuring of the Au nanoparticles induced by the adsorbed Nip. The rate $1/t_0$ of this substrate-induced surface restructuring is found to be proportional to the square of the surface coverage, θ_{Nip}, by Nip and therefore points to a cooperative process.

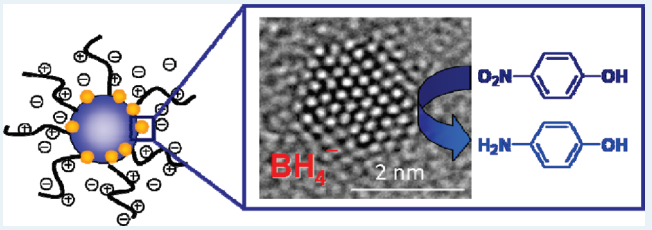

KEYWORDS: catalysis, nanoparticles, Langmuir−Hinshelwood kinetics, surface restructuring

INTRODUCTION

Catalysis by metallic nanoparticles has become an area of intense research in recent years.[1,2] Thus, metals that are inactive in the bulk state—for example, gold—become active catalysts when dispersed down to the nanoscale.[3,4] Nanoparticles of noble metals are easily generated in aqueous solution, and redox reactions proceeding under these conditions can be used to assess their catalytic activity.[5−7] Here, a precise kinetic analysis is very useful, since it allows one to correlate the size and the shape of the particles to their catalytic properties in a quantitative manner. However, this type of analysis can be done only for model reactions, that is, for chemical reactions that proceed in a well-defined manner from a single educt to a single product. Monitoring the model reaction should be possible in a precise way. Moreover, a change of temperature should not lead to a change in the mechanism or to undesired side reactions. Because most of the catalytic reactions take place on the surface area of the particles, their total surface should be characterized with sufficient accuracy. In addition, the nanoparticles must exhibit sufficient colloidal stability, coagulation of the nanoparticles, or further chemical transformations such as dissolution should not occur.

As shown first by Pal and co-workers[8] and by Esumi et al.,[9] the reduction of *p*-nitrophenol (Nip) to *p*-aminophenol (Amp) by borohydride ions (BH_4^-) qualifies as such a model reaction. There is no side reaction, and the progress of the reaction can be easily followed by UV−vis spectroscopy. An excess of BH_4^- is often applied, and the decrease in the strong UV−vis adsorption of Nip at 400 nm wavelength is treated in terms of a first-order reaction. The rate k_{app} of the decay of Nip thus defined has been used repeatedly to compare the catalytic activity of various nanoparticulate systems.[8−43] In this way, the reduction of Nip has become perhaps the most-studied reaction for investigating the catalytic activity of nanoparticles, and the number of papers devoted to this reaction is steadily increasing.

Recently, the dependence of the rate constant of this reaction on temperature has moved into the focus of research.[14,17−35] The activation energy, E_A, can be derived easily from the respective Arrhenius plots of k_{app} and related to structural parameters of the nanoparticles. The data derived from this analysis then can be

Received: April 20, 2011
Revised: May 26, 2011
Published: June 20, 2011

used to discuss the influence of the shape and morphology of the nanoparticles on their catalytic activity. In particular, recent work has demonstrated that the frequency factor derived from the intercept of the Arrhenius plot is directly related to E_A.[26,28,34] A kinetic model for this reaction must explain this important finding.

Here, we analyze the dependence of the reduction of *p*-nitrophenol by borohydride as a function of temperature. The analysis presented here is based on our finding that the kinetics of this model reaction can be treated in terms of the Langmuir−Hinshelwood (LH) model:[35] Both reactants must be adsorbed to the surface of the particles to react. The adsorption of both educts is modeled in terms of an equilibrium process described by the classical Langmuir isotherm. The adsorbed species can then react, and the product dissociates from the surface. This model was shown to give an excellent description of the kinetics of this model reaction.[35] In particular, it explains two effects not expected for a reaction in solution: The apparent kinetic constant, k_{app}, decreases with increasing concentration of Nip and goes through a shallow maximum as with increasing concentration of BH_4^-. Within the frame of the LH model, these observations can be modeled through a competition of both reacting species for surface sites suitable for adsorption. The analysis of the kinetic data in terms of the LH model yields the true kinetic constant k of the surface reaction together with the thermodynamic adsorption constants K_{Nip} and K_{BH_4} for both Nip and BH_4^-, respectively. The dependence of the overall rate constant k_{app} of the reduction on temperature is therefore given by three terms: namely, the activation energy of the surface reaction and the enthalpies of adsorption of both species. Evidently, the apparent activation energy, E_A, obtained from the temperature dependence of k_{app} cannot be discussed solely in terms of a purely kinetic model, but must comprise the analysis of the thermodynamics of adsorption, as well.

An important feature of the reduction of Nip catalyzed by nanoparticles is the induction time, t_0, which can take up to several minutes. As observed for a number of systems, the reaction starts only after this induction time, and various models have been proposed to explain this fact.[8,14,26,34,35,37−42] In an important paper, Zhou et al. measured induction periods of similar magnitude for Au nanoparticles in a different reaction[44] and explained it by the restructuring of the surface by the reactants. Adsorbate-induced restructuring of the metal surface is a well-established concept in catalysis[45,46] that has been observed for many systems in the gaseous phase. The detailed analysis in ref 35 suggested that induction time t_0 is related to a restructuring of the surface by Nip. A more detailed understanding of the dependence of the reaction on temperature must therefore comprise an analysis of t_0 as the function of temperature, as well.

The analysis performed here uses gold nanoparticles affixed to the surface of spherical polyelectrolyte brushes (SPB[47]) as catalysts.[15,35,36] Figure 1 displays schematically the structure of these composite particles: Cationic polyelectrolyte chains are densely grafted to the surface of colloidal polystyrene spheres with a diameter of ∼100 nm. The Au nanoparticles are generated in the surface layer of polyelectrolyte chains as described recently.[15,35,36] These composite particles consisting of the SPB and the metallic nanoparticles exhibit an excellent colloidal stability. A number of previous studies have revealed that these composite particles can be used for the quantitative study of the kinetics of the reduction of Nip in the presence of metal nanoparticles.[14−17,31,35]

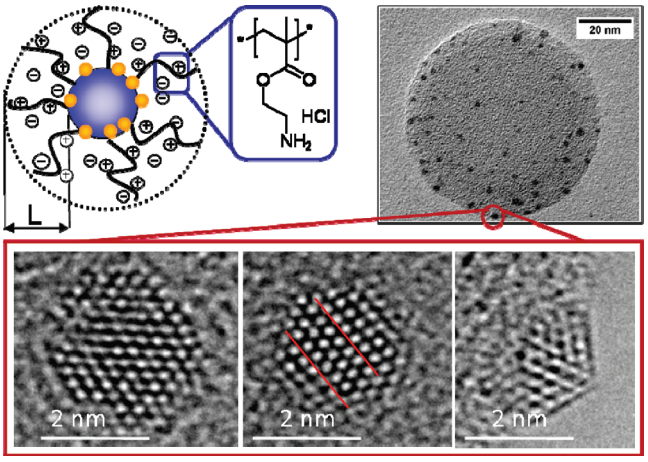

Figure 1. Structure of the composite particles used in the kinetic studies. Upper panel, left-hand: Scheme of the composite particles consisting of spherical polyelectrolyte brushes (SPB) and gold nanoparticles. Au NP were generated in a SPB consisting of poly([2-aminoethyl]-methacrylate hydrochloride) chains that were attached on polystyrene cores with a diameter of 88 ± 5 nm. The thickness of the layer of the polyelectrolyte chains (L) was 66 ± 7 nm as determined through dynamic light scattering. Upper panel, right side: TEM micrograph of a composite particle. Lower panel: High-resolution electron microscopy (HR-TEM) micrograph of faceted gold nanoparticles on a SPB consisting of polystyrene and poly[2-aminoethyl]-methacrylate hydrochloride. The central one shows a twin marked by red lines.

The aim of the present work is two-fold: (i) We aim at an in-depth understanding of the various contributions to the apparent activation energy, E_A, that has previously been obtained by the Arrhenius-analysis of k_{app}, and (ii) we wish to elucidate the origins of the induction period, t_0. Special emphasis is laid on the structure of the nanoparticles, since the entire analysis is related to their surface. The present data will demonstrate that a full mechanistic analysis of a model reaction catalyzed by nanoparticles becomes possible using these composite systems.

EXPERIMENTAL SECTION

The spherical polyelectrolyte brushes (SPB; cf. Figure 1) were obtained and characterized as described recently.[36] The cores of the composite particles had a diameter of 88 ± 5 nm, whereas the thickness of the brush layer (L) was evaluated with 66 ± 7 nm, determined by dynamic light scattering. The composites of spherical polyelectrolyte brushes and gold nanoparticles were synthesized as described previously.[15,35] After the synthesis of the gold NP, the brush thickness decreased to 43 ± 3 nm, as determined by dynamic light scattering. This points to a strong interaction of the nanoparticles with the polyelectrolyte chains as already discussed in ref 36. In a typical experiment, 10 mL of an aqueous solution of 2.55 mM metal salt was added dropwise to 0.1 g of latex in 100 mL. Afterward the solution was purged with N_2 to remove the oxygen, then a 3-fold excess of sodium borohydride was slowly added to reduce the metal ions. After the reduction was finished, the sample was cleaned by ultrafiltration.

The overall size of the Au NP was measured with transmission electron microscopy (Phillips CM30). Approximately 600 particles were counted, and the average size was calculated to be 2.2 ± 0.4 nm. The high-resolution transmission microscopy (HR-TEM) studies of single particles were performed using an objective lens corrected FEI Titan 80-300 operated at 300 keV.

dx.doi.org/10.1021/cs200208a |*ACS Catal.* 2011, 1, 908–916

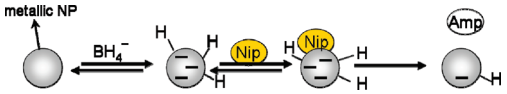

Figure 2. Langmuir−Hinshelwood mechanism of the reduction of *p*-nitrophenol by borohydride on the surface of metallic nanoparticles (gray spheres). The catalytic reduction proceeds on the surface of the metal nanoparticles: Borohydride ions react with the surface of the nanoparticles to form a surface-hydrogen species. Concomitantly, *p*-nitrophenol adsorbs onto unoccupied sites of the metal surface. The adsorption/desorption of both reagents on the surface is fast and is modeled in terms of a Langmuir isotherm. The rate-determining step is the reduction of the adsorbed Nip to Amp, which desorbs afterward.[35]

The aberration corrector was set to small negative values, c_s < 200 nm. Images were taken at Gaussian focus or small positive focus values. The amount of metal inside the SPBs was measured by TGA using a Netsch STA 409PC LUXX. Fifteen milligrams of dried sample was heated to 800 °C under a constant argon flow (30 mL/min) with a heating rate of 10 K/min. The specific surface area of the nanoparticles was calculated from the average radius obtained from the TEM micrographs, and the total mass per particle was calculated from the TGA measurements. The specific surface thus was calculated with 0.0108 m^2/L.

The kinetic measurements were performed in a 3 mL quartz cell using a Lambda 650 spectrometer from Perkin-Elmer. The solutions of BH_4^- and Nip were freshly prepared before each measurement, then purged with N_2, mixed together with a given amount of catalyst, and placed in the spectrometer. The extinction of Nip was subsequently detected at a constant pH value of 10 at λ = 400 nm. The reaction was monitored at four different temperatures (10, 20, 25, and 30 °C). The weight percent of gold is 7.7×10^{-7} wt % in the final system used for the catalytic runs.

KINETIC ANALYSIS

The analysis of the kinetic data was done in terms of the Langmuir−Hinshelwood model.[35] Figure 2 displays the essential assumptions of this model. Borohydride ions react with the surface of the nanoparticles and transfer a surface-hydrogen species to the surface of the particles.[48,49] Previous work suggests that this step is reversible and can be modeled in terms of a Langmuir isotherm.[35] It should be kept in mind, however, that the interaction of borohydride ions with metallic surfaces is a complicated process that comprises several steps.[48,49] The treatment of this step in terms of a Langmuir isotherm is a simplification that finds justification in the subsequent analysis. At the same time, Nip molecules are adsorbed onto the surface of the nanoparticles. This step is certainly reversible and can be modeled by a Langmuir isotherm.[35,50] Furthermore, it is assumed that the diffusion of the reactants to the nanoparticles as well as all the adsorption/desorption steps are fast. The reduction of Nip adsorbed on the surface with the surface hydrogen species is the rate-determining step. The final step of the catalytic cycle (namely, the detachment of the product Amp) is also fast and therefore does not enter into the kinetic equations.[35]

Within the LH model, the apparent kinetic rate constant, k_{app}, is strictly proportional to the total surface, S, of all metal nanoparticles, and the kinetic constants k_{app} and k_1 can be defined through[35]

$$\frac{dc_{Nip}}{dt} = -k_{app} \cdot c_{Nip} = -k_1 \cdot S \cdot c_{Nip} \quad (1)$$

The LH model implies that

$$\frac{dc_{Nip}}{dt} = -kS\theta_{Nip}\theta_{BH_4} \quad (2)$$

where θ_{Nip} and θ_{BH_4} denote the surface coverage of the nanoparticles by Nip and borohydride, respectively, and k is the rate constant of the surface reaction. They are modeled by a Langmuir isotherm,

$$\theta_{Nip} = \frac{(K_{Nip}c_{Nip})^n}{1 + (K_{Nip}c_{Nip})^n + K_{BH_4}c_{BH_4}} \quad (3a)$$

$$\theta_{BH_4} = \frac{K_{BH_4}c_{BH_4}}{1 + (K_{Nip}c_{Nip})^n + K_{BH_4}c_{BH_4}} \quad (3b)$$

Here, K_{Nip} and K_{BH_4} are the adsorption constants of Nip and BH_4^-, respectively, and c_{Nip} and c_{BH_4} denote the respective concentrations in solution. The exponent n is related to the heterogeneity of the sorbent.[51] It takes into account that the adsorption energy of the adsorption sites is not homogeneous and can be modeled by a Gaussian distribution. Previous work has shown that the adsorption of Nip is best modeled by assuming an exponent n = 0.6, whereas the adsorption of borohydride can be described through the classical Langmuir isotherm with n = 1.[35] With these definitions, eq 1 can be rewritten as

$$-\frac{dc_{Nip}}{dt} = \frac{k \cdot S \cdot (K_{Nip} \cdot c_{Nip})^n \cdot K_{BH_4} \cdot c_{BH_4}}{\left(1 + (K_{Nip} \cdot c_{Nip})^n + K_{BH_4} \cdot c_{BH_4}\right)^2} = k_{app} \cdot c_{Nip} \quad (4)$$

Therefore, k_{app} follows as

$$k_{app} = \frac{k \cdot S \cdot K_{Nip}^n \cdot c_{Nip}^{n-1} \cdot K_{BH_4} \cdot c_{BH_4}}{\left(1 + (K_{Nip} \cdot c_{Nip})^n + K_{BH_4} \cdot c_{BH_4}\right)^2} \quad (5)$$

Equation 5 demonstrates that the true rate constant, k, which is related to the reaction of the adsorbed species, can be obtained from a fit of k_{app} to the experimental data if the total surface area, S, of the particles is known. Moreover, this analysis leads to the adsorption constants K_{Nip} and K_{BH_4}.

The dependence of the rate constants k and k_{app} on temperature, T, can be expressed through the Arrhenius equation

$$k = k_0 \, exp\left(-\frac{E_{A,k}}{RT}\right) \quad (6a)$$

$$k_{app} = k_{app,0} \, exp\left(-\frac{E_A}{RT}\right) \quad (6b)$$

where k_0 is the frequency factor of the surface reaction and $E_{A,k}$ defined through eq 6a is the true activation energy of the surface reaction. It should not be confused with the apparent activation energy, E_A, obtained from an analysis of k_{app} according to eq 6b.

As shown by eq 5, k_{app} contains the temperature dependence not only of k but also of K_{Nip} and K_{BH_4}. Since these adsorption constants can now be obtained as a function of temperature, the enthalpies ΔH_{Nip} and ΔH_{BH_4} for the adsorption of Nip and

dx.doi.org/10.1021/cs200208a |ACS Catal. 2011, 1, 908–916

BH_4^- can be obtained from the application of van't Hoff's equation:

$$\frac{\mathrm{d}\, ln\, K}{\mathrm{d}(1/T)} = -\frac{\Delta H}{R} \quad (7)$$

With these values, the entropy of adsorption ΔS_{Nip} and ΔS_{BH_4} can be calculated according to

$$ln\, K = -\frac{\Delta G}{RT} = -\frac{\Delta H}{RT} + \frac{\Delta S}{R} \quad (8)$$

A central prerequisite of the above analysis is the assumption that the reaction of the adsorbed species constitutes the rate-determining step. This implies that the diffusion of the reactants to and from the nanoparticles is much faster than the chemical reaction on their surface. This is different from the oxidation reaction on the surface of Au nanoparticles studied by Carregal-Romero et al.,[52] which was shown to be limited by the diffusion of the reactants. For the reaction under consideration here, control by diffusion can be definitely ruled out by calculating the second Damköhler number (DaII), which assesses the competition between the chemical reaction and mass transport through diffusion:[53]

$$DaII = \frac{k \cdot c^{n-1}}{\beta \cdot a} \quad (9)$$

where k is the reaction rate constant, c is the concentration, n is the reaction order (here, first order), β is the mass transport coefficient, and a is the total area of the interface. In general, β is given by the diffusion coefficient divided by characteristic length scale, δ, over which mass transport takes place.[53] For a conservative estimate of β, it is expedient to use the thickness of the entire brush layer as the magnitude of δ, assuming that the brush layer does not disturb the diffusion of the reactants. For the present system, δ = 40 nm. The interfacial area, a, is 10.78 1/m and the diffusion coefficient of Nip is given by $6.92 \cdot 10^{-10}$ m^2/s (water, 20 °C; taken from ref 54). Hence, β is given by 0.0173 m/s. As for the rate constant, the value of 0.00149 1/s, which has been derived for 10 mM BH_4^- and 0.1 mM Nip,[35] could be used for an estimate of DaII. From these figures, DaII follows as 8×10^{-3}, which is far below unity. Since a more realistic value of δ is on the order of a nanometer only, a better estimate of DaII is on the order of 10^{-4}. Moreover, this estimate is based on the assumption of a planar system. However, mass transport takes place around strongly curved nanoparticles. In this case, the radial symmetry leads to a much faster mass transport. Evidently, mass transport in the present system is faster by at least 2 orders of magnitude, and it can be safely stated that there is no diffusion control. This conclusion is also important for the discussion of t_0, since it demonstrates that the induction time found for the present system is not due to diffusional barriers.

RESULTS AND DISCUSSION

As in previous papers, we use spherical polyelectrolyte brushes as carriers for the nanoparticles.[14−17,31,35,36,47] The SPB used here carry long chains of the cationic polyelectrolye poly-[(2-aminoethyl)methacrylate hydrochloride] (see Figure 1). These particles have been shown to be excellent carriers for the Au nanoparticles recently because of their stability against coagulation or Ostwald ripening.[15,35,36,47] The average size of the Au nanoparticles was found to be 2.2 ± 0.4 nm, as derived from TEM micrographs (see Figure 1). The total surface area, S, of the nanoparticles present in the system can be calculated and used in the analysis of the kinetic data. Moreover, the Au nanoparticles present a well-defined catalyst, as shown here by HR-TEM: Figure 1 demonstrates that these nearly monodisperse Au nanoparticles are well-defined truncated octahedral metallic nanocrystals bound by {111} and {100} facets. Hence, the catalysis performed with these particles can be compared in many respects with catalytic studies done on well-defined macroscopic surfaces.[46]

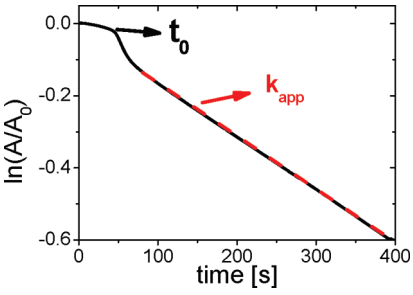

Figure 3. Time dependence of the absorption of *p*-nitrophenolate ions at 400 nm shown for a typical run (c_{Nip}, 0.1 mM; c_{BH_4}, 5 mM; S, 0.0108 m^2/L; T, 25 °C). The red section of the line displays the linear section from which k_{app} was taken. The induction time, t_0, is marked by an arrow.

Figure 3 shows the typical time dependence of the reduction of Nip at a wavelength of 400 nm. As already discussed in previous work, there is an induction time, t_0, in which no reduction takes place.[14,35] Then the reaction becomes stationary, and the reaction follows a first-order rate law. Similar plots have been found by a number of other authors.[10,13,14,17,19,21,22,24,26,31−33,35,38,39,42] From this linear part, the reaction rate constant, k_{app}, was taken. In the following, we shall first discuss the stationary part of the reaction and analyze k_{app}. In a second part, t_0 will be analyzed as the function of the temperature.

Kinetic Constant, k_{app}, for the Steady State of the Reaction. For the kinetic analysis, two sets of experiments were run at four different temperatures: first, the varying of the Nip concentrations at constant concentrations of BH_4^- (10 and 5 mM), and in a second setup of experiments, the concentration of BH_4^- was varied while the concentration of Nip was set constant (0.1 and 0.05 mM). Figure 4 shows the k_{app} as a function of the concentrations of either Nip (a, b) or BH_4^- (c, d) at different temperatures. The lines are the corresponding fits from the Langmuir−Hinshelwood model. The respective fit parameters are summarized in Table 1. As shown in Figure 4 an increase in the concentration of Nip always leads to a decrease in the rate constant (k_{app}). On the other hand, an increase in the concentration of BH_4^- leads to an increase in the reaction rate, which levels off at the highest concentrations. The explanation for this characteristic dependence of k_{app} on the concentrations of both reactants has already been given previously.[35] Both reactants compete for free places at the surface of the Au nanoparticles, and the reaction can occur only between species adsorbed on the surface. If most places are occupied by a single species, the reaction will be slowed down considerably. This is seen for higher concentrations of Nip that strongly adsorbs to the surface of the Au nanoparticles and thus blocks the surface reaction.

By measuring the reaction at different temperatures, the adsorption constants K_{Nip} and K_{BH_4} can be determined as a function of temperature (see Table 1). The adsorption constant K_{Nip} of Nip increases with an increasing temperature (Figure 5a),

dx.doi.org/10.1021/cs200208a |ACS Catal. 2011, 1, 908–916

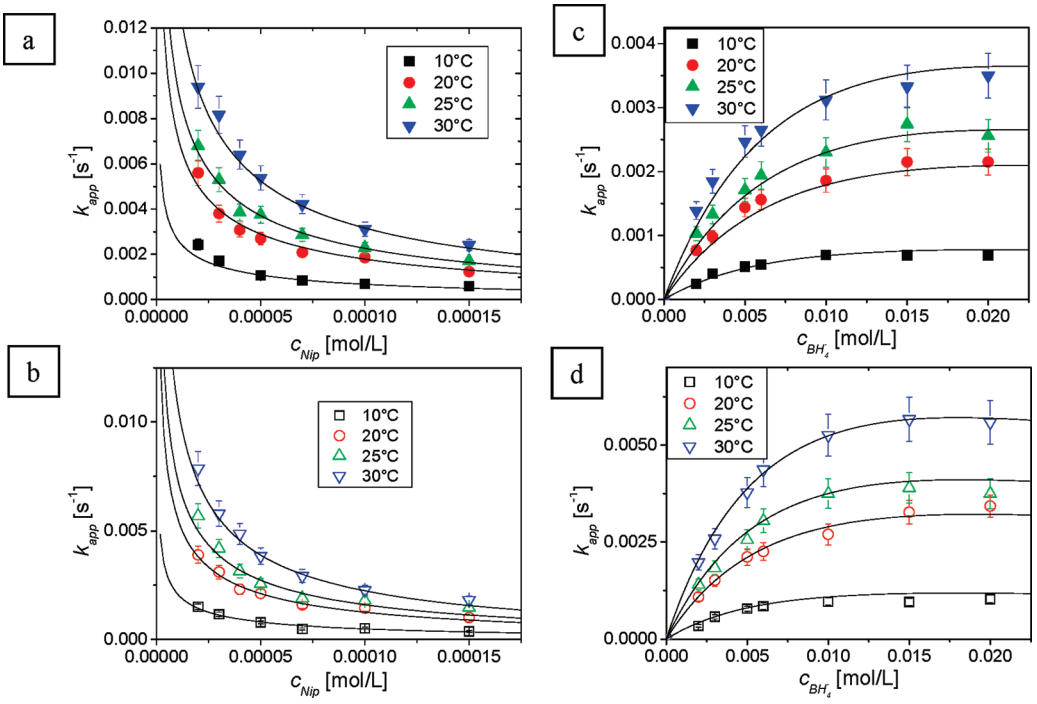

Figure 4. Dependence of the apparent rate constant, k_{app}, on the concentration of Nip at constant concentrations of BH_4^- (10 mM in a, 5 mM in b) and on the concentration of BH_4^- at a constant concentrations of Nip (0.1 mM in c, 0.05 mM in d) at different temperatures. Black lines are the Langmuir−Hinshelwood fits for the different temperatures. The surface of the nanoparticles in the reaction volume was calculated to 0.0108 m^2/L.

Table 1. Summary of the Rate Constants, *k*, and the Adsorption Constants of Nip and BH_4^- (K_{Nip} and K_{BH_4}) at Different Temperatures by Fitting the Experimental Data with Langmuir-Hinshelwood Shown in Figure 4

T	10 °C	20 °C	25 °C	30 °C
k (mol/m^2 s)	$(0.73 \pm 0.10) \cdot 10^{-4}$	$(1.89 \pm 0.28) \cdot 10^{-4}$	$(2.27 \pm 0.34) \cdot 10^{-4}$	$(2.92 \pm 0.44) \cdot 10^{-4}$
K_{Nip} (L/mol)	5300 ± 800	5900 ± 900	6400 ± 1000	7800 ± 1200
K_{BH_4} (L/mol)	79 ± 12	76 ± 11	82 ± 12	87 ± 13
n	0.6 ± 0.1	0.6 ± 0.1	0.6 ± 0.1	0.6 ± 0.1

whereas the change of K_{BH_4} is smaller in the same temperature range. Table 2 summarized the respective thermodynamic parameters of both compounds. In the case of Nip, the adsorption is endothermic. The positive value of ΔS indicates that the liberation of water or other surface-bound species is the dominating process of adsorption.

In contrast, the adsorption constant of BH_4^- (Figure 5b) is much smaller. As mentioned above, the interaction of BH_4^- ions with metal surfaces is a complicated process that involves several steps.[48,49] For the present analysis, it suffices to note that the analysis of k_{app} allows a full description of the experimental data for the entire range of temperatures under consideration here.

Table 1 shows that the surface rate constant, k, is increasing with temperature and the activation energy, $E_{A,k}$, result is 49 kJ/mol from the respective Arrhenius plot (Figure 6). This value is in the same range as that of k_{app} (50 kJ/mol) measured at 0.1 mM Nip and 10 mM BH_4^-, where both concentrations are near their plateau values (see Figure 4). However, $E_{A,k}$ is a true activation energy that is related to a kinetic rate constant; namely, to the one related to the reaction of the surface-bound species with adsorbed Nip. The activation energy obtained from k_{app} is only an apparent value, since it contains the temperature dependence of the adsorption constants K_{Nip} and the adsorption constants K_{BH_4}, as well.

This point can be elucidated further by Arrhenius plots of k_{app} referring to various concentrations of Nip at 10 mM BH_4^-. From Figure 6a, apparent activation energies, E_A, were calculated to be in the range between 49 and 57 kJ/mol. Moreover, a plot of the corresponding frequency factors, k_0, calculated from the Arrhenius plot as a function of the apparent activation energies leads to a linear relation (compensation law plot; cf. ref 28). Figure 6b assembles all data obtained here and from previous work for different metal nanoparticles.[14,17,31,35] This compensation effect has be explained by the following effects:[55] (1) heterogeneity of activity and distribution of active sites,[56] (2) entropy-enthalpy relation,[56,57] (3) relation between the coverage of the surface and activation energy,[56,58] (4) selective energy transfer,[59] and (5) correlation of the activation energy of the rate-determining step and the stability of the reaction intermediates.[60]

For the present system, an explanation can be given as follows: As shown in Figure 6b, a linear compensation can be found for activation energies and frequency factors of different nanoparticles embedded in SPB. In particular, the data obtained for the present system can be described by this type of compensation plot. On the other hand, the above analysis has shown that all kinetic data are fully compatible with the Langmuir−Hinshelwood model. Thus, the compensation can be explained by the

dx.doi.org/10.1021/cs200208a |*ACS Catal.* 2011, 1, 908–916

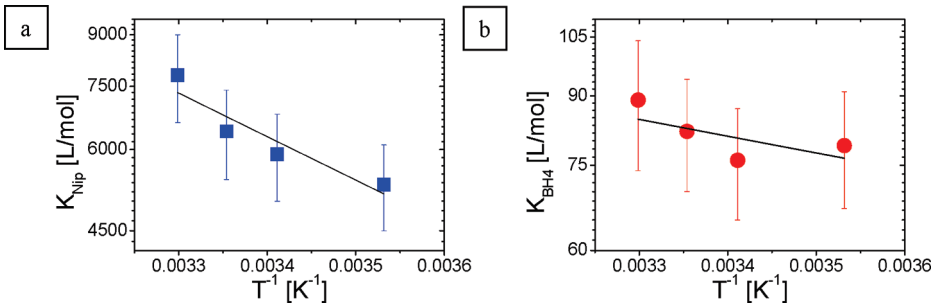

Figure 5. Dependence of the adsorption constants K_{Nip} of Nip (a) and the adsorption constants K_{BH_4} of borohydride (b) on the inverse temperature. The enthalpies of the adsorption process were calculated from these plots using the van't Hoff's equation. From this, the entropies can be obtained. All values are given in Table 2.

Table 2. Summary of Enthalpy and Entropy Values of the Adsorption Process of Nip and BH_4^-

	K_{Nip}	K_{BH_4}
ΔH [kJ/mol]	13 ± 4	3.3 ± 2.6
ΔS [J/mol K]	116 ± 11	46 ± 9

different surface coverage, θ, of the metal nanoparticles at different temperatures.[56,58] To verify this, we calculated the rate constants $k_{1,\theta}$ at given constant coverage but at different temperatures. The respective plots of $k_{1,\theta}$ are shown in Figure S2 in the Supporting Information. As expected from the LH analysis, the resulting activation energies are approximately the same (60 kJ/mol) for a constant surface coverage; only the frequency factors change. It thus becomes obvious that the compensation law is a natural consequence of the LH kinetics and can be traced back to a change in the surface coverage by changing the temperature.

The influence of the thermodynamic adsorption parameters on k_{app} can be seen directly from eq 5 for the limiting case of small concentrations of both reactants. In this case, the denominator of the term referring to adsorption is unity, and the measured activation energy is modified by terms that contain the adsorption enthalpy. The preexponential factor, in turn, contains terms that depend on the adsorption entropy. Since ΔH_{Nip} and ΔS_{Nip} are positive for the present system, both the apparent preexponential factor and the apparent activation energy will increase. If, on the other hand, the concentration of both reactants is high, the surface of the nanoparticles is saturated. Thus, the influence of the adsorption terms will nearly cancel out in eq 5. The activation energy measured from k_{app} is therefore dominated by $E_{A,k}$, and the preexponential factor, by k_0.

Induction Period, t_0. As shown in Figure 3, the reaction starts only after an induction period, t_0. As discussed in previous work, the induction is nearly independent of the concentration of BH_4^- (see Figure S1); however, it depends strongly on the concentration of Nip.[35] Here, it is argued that the induction time is due to a substrate-induced surface restructuring that is necessary to render the metal nanoparticles an active catalyst. To pursue this problem in further detail, the induction time is treated as a rate constant and plotted against the concentration of Nip, as shown in Figure 7a. An intercept $(1/t_{0,sp})$ at $c(\text{Nip}) = 0$ can be clearly seen in this plot, which must be caused by a spontaneous surface reconstruction of the Au NP that occurs in the absence of a substrate. In addition, measurements at different

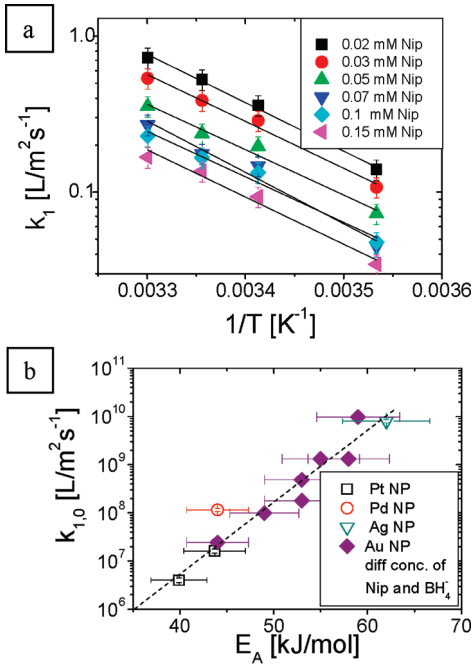

Figure 6. (a) Arrhenius analysis of the kinetic constants obtained in the present analysis. Arrhenius plot of the rate constant k_1 (k_{app} normalized to the total surface S of the nanoparticles; cf. eq 1) for different concentrations of Nip at 10 mM BH_4^-. (b) Compensation plot of the frequency factors $k_{1,0}$ (cf. eqs 6a, 6b) vs the apparent activation energies, E_A, obtained from panel a for different metallic nanoparticles embedded in SPBs. Solid symbols indicate the data for selected concentrations of nitrophenol and BH_4^- from this work (see also Table S1), whereas open symbols present data taken from the literature: Platinum nanoparticles (Pt NP), refs 14 and 35. Palladium nanoparticles (Pd NP), ref 17; silver nanoparticles (Ag NP), ref 31.

temperatures lead to an activation energy of this spontaneous surface reconstruction with 55 kJ/mol (Figure 7b). These findings are very similar to those of Zhou et al.,[44] who studied the reduction of reazurin with hydroxylamine on Au nanoparticles by an optical technique. The evidence for substrate-induced surface restructuring was found from a similar analysis (see Figure 6 of ref 44). In this work, the activation energy for the spontaneous surface restructuring of gold nanoparticles was found to be 19 kJ/mol. This value is lower than the activation energy we have determined here, and the difference may arise from the different size of the nanoparticles used in the work of Zhou et al.[44]

dx.doi.org/10.1021/cs200208a |ACS Catal. 2011, 1, 908–916

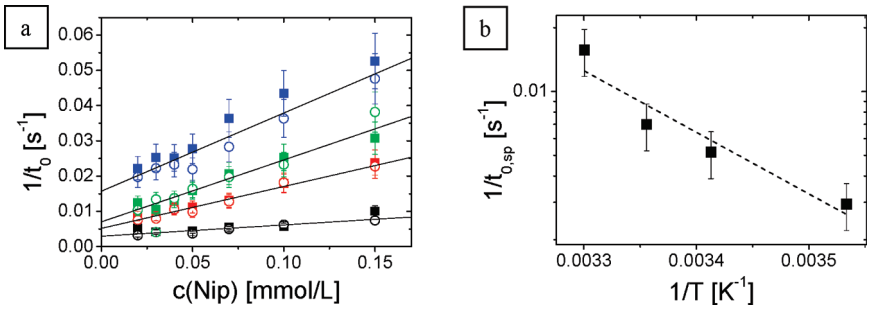

Figure 7. Analysis of the delay time, t_0. Left-hand side: The dependence of the inverse induction time as a function of the concentration of Nip. The solid squares are at a concentration of 10 mM BH_4^-, and the open circles are at a concentration of 5 mM BH_4^-. The temperatures are as follows: black, 10 °C; red, 20 °C; green, 25 °C; and blue, 30 °C. Right-hand side: The temperature dependence of the intercept of $1/t_0$. The activation energy can be calculated as 55 ± 9 kJ/mol.

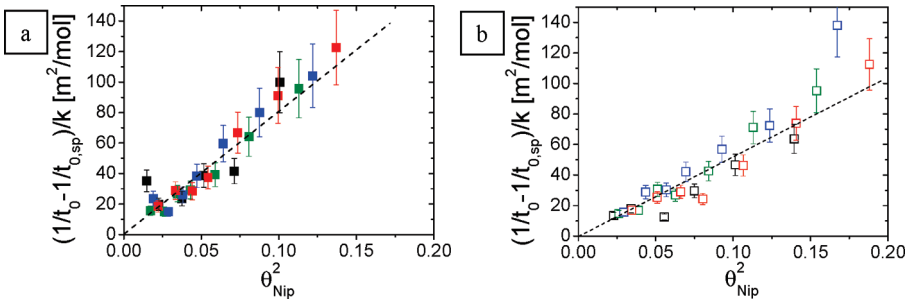

Figure 8. Relation of the substrate-induced surface restructuring to the coverage of the nanoparticles by the substrate nitrophenol. Dependence of $((1/t_0) - (1/t_{0,sp}))/k$ to the surface coverage, θ_{Nip}, of nitrophenol at a concentration of BH_4^- of 10 mM (a), and 5 mM (b), respectively. The temperatures are as follows: black, 10 °C; red, 20 °C; green, 25 °C; and blue, 30 °C.

In the following the rate of the substrate-induced surface restructuring given by $(1/t_0) - (1/t_{0,sp})$ will be discussed. The previous analysis[35] has suggested that this rate is related to the rate constant, k, of the stationary reaction. The present data fully corroborate this conjecture by using data referring to different temperatures: Figure 8 displays the rate of substrate-induced surface restructuring normalized to k; that is, $((1/t_0) - (1/t_{0,sp}))/k$ as a function of the square of the surface coverage θ_{Nip}^2. All data superimpose to a master curve, and a linear relationship is obtained within the experimental limits of error. The concentration of borohydride was kept constant in both panels. Note that both panels contain data referring to different temperatures. Clearly, the temperature dependence of $(1/t_0) - (1/t_{0,sp})$ is fully governed by the temperature dependence of k. The influence of the borohydride concentration is marginal, since the slope of the straight lines in Figure 8a and b differ only slightly.

Figure 8 presents the key result for the present analysis of the induction time, t_0. It demonstrates that (i) the rate of substrate-induced restructuring $(1/t_0) - (1/t_{0,sp})$ is solely related to the surface coverage, θ_{Nip}, and (ii) the dependence on θ_{Nip} is quadratic; that is, at least two Nip molecules should interact to induce the change of surface structure. The restructuring of metal surfaces by substrates is a well-known effect in catalysis. Small molecules are known to lift the reconstructed Au surface, even at low temperatures.[61−63] In an adsorption study of CO molecules on a gold surface, Pierce et al.[64] found that the restructuring rate of the gold surface is dependent on the amount of adsorbed CO molecules. Driver et al.[61] found that lifting of the reconstruction by adsorption of NO molecules is a concerted process: once a critical island size of adsorbed NO molecules is reached, a cooperative restructuring occurs. A similar effect was found for adsorbate-induced restructuring of the surface of Pt surfaces.[65,66] Clearly, no direct evidence can be given for the present system yet, since an analysis of the surface of single nanoparticles with the required accuracy is still a formidable task. However, the evidence given here is in full accord with the similar findings of Zhou et al.[44] Thus, we are led to the conclusion that the Au nanoparticles under consideration here require a reconstruction of the surface to become active catalysts.

CONCLUSIONS

The catalytic reduction of nitrophenol with sodium borohydride and its dependence on temperature can be fully described by the Langmuir−Hinshelwood model in which both reactants are adsorbed on the surface of the nanoparticles. The reaction can be described with 3 constants: the intrinsic rate constant, k; the adsorption constants for nitrophenol, K_{Nip}; and borohydride, K_{BH_4}. Analysis of these constants as the function of temperature leads to the true activation energy of $E_{A,k}$ = 49 kJ/mol of the true rate constant, k. The dependence of the constants K_{Nip} and K_{BH_4} on temperature could be evaluated to obtain the adsorption enthalpy and entropy for both reactants. The induction period, t_0, was traced back to surface restructuring of the nanoparticles, and any limitation by diffusion could be clearly ruled out. The analysis of t_0 as a function of the concentration of nitrophenol revealed evidence for two restructuring processes: one spontaneous process (see the discussions of the intercepts in Figure 7a) and one process that depends on the square of the surface coverage θ_{Nip} of the substrate nitrophenol. The rate of this

dx.doi.org/10.1021/cs200208a |ACS Catal. 2011, 1, 908–916

substrate-induced surface restructuring was found to be directly related to the rate, k, of the surface reaction as revealed by the Langmuir−Hinshelwood ansatz eq 5. Scaling of this rate leads to a master curve in which all data superimpose when plotted against $\theta_{Nip}{}^2$ (see Figure 8). Hence, the reduction of nitrophenol with borohydride cannot take place on the surface of pristine nanoparticles, but requires a surface restructuring that seems to be a cooperative process involving several nitrophenol molecules. In this respect, catalysis on the surface of Au nanoparticles seems to follow the mechanisms that have been firmly established for macroscopic surfaces in recent years.[45,46]

■ ASSOCIATED CONTENT

Supporting Information. Additional information as noted in the text. This information is available free of charge via the Internet at http://pubs.acs.org/.

■ AUTHOR INFORMATION

Corresponding Author
*E-mail: matthias.Ballauff@helmholtz-berlin.de.

■ ACKNOWLEDGMENT

Financial support by the Deutsche Forschungsgemeinschaft is gratefully acknowledged.

■ REFERENCES

(1) Astruc, D. *Nanoparticles and Catalysis*; Wiley-VCH: Weinheim, 2008.
(2) Saradar, R.; Funston, M. A.; Mulvaney, P.; Murray, R. W. *Langmuir* **2009**, *25*, 13840–13851.
(3) Hashmi, A. S.; Hutchlings, G. *J. Angew. Chem. Int. Ed.* **2006**, *45*, 7896–7936.
(4) Hutchlings, G. J; Brust, M.; Schmidbaur, H. *Chem. Soc. Rev.* **2008**, *37*, 1759–1765.
(5) Pina, C. D.; Falletta, E.; Prati, L.; Rossi, M. *Chem Soc Rev.* **2008**, *37*, 2077–2095.
(6) Gong, J.; Mullins, C. B. *Acc. Chem. Res.* **2009**, *42*, 1063–1073.
(7) Corma, A.; Garcia, H. *Chem. Soc. Rev.* **2008**, *37*, 2096–2126.
(8) Pradhan, N.; Pal, A.; Pal, T. *Colloids Surf., A* **2002**, *196*, 247–257.
(9) Esumi, K.; Miyamoto, K.; Yoshimura, T. *J. Colloid Interface Sci.* **2002**, *254*, 402–405.
(10) Xia, Y.; Xiao, H. *J. Mol. Cat. A: Chem.* **2010**, *331*, 35–39.
(11) Tang, S.; Vongehr, S.; Meng, X. *J. Mater. Chem.* **2010**, *20*, 5436–5445.
(12) Jana, D.; Dandapat, A.; De, G. *Langmuir* **2010**, *26*, 12177–12184.
(13) Ballarin, B.; Cassani, M. C.; Tonelli, D.; Boanini, E.; Albonetti, S.; Blosi, M.; Gazzano, M. *J. Phys. Chem. C* **2010**, *114*, 9693–9701.
(14) Mei, Y.; Sharma, G.; Lu, Y.; Ballauff, M.; Drechsler, M.; Irrgang, T.; Kempe, R. *Langmuir* **2005**, *21*, 12229–12234.
(15) Lu, Y.; Wittemann, A.; Ballauff, M. *Macromol. Rapid Commun.* **2009**, *30*, 806–815.
(16) Schrinner, M.; Ballauff, M.; Talmon, Y.; Kauffmann, Y.; Thun, J.; Möller, M.; Breu, J. *Science* **2009**, *323*, 617–620.
(17) Mei, Y.; Lu, Y.; Polzer, F.; Ballauff, M. *Chem. Mater.* **2007**, *19*, 1062–1069.
(18) Panigrahi, S.; Basu, S.; Praharaj, S.; Pande, S.; Jana, S.; Pal, A.; Gosh, S. K.; Pal, T. *J. Phys. Chem. C* **2007**, *111*, 4596–4605.
(19) Chen, X.; Zhao, D.; An, Y.; Zhang, Y.; Cheng, J.; Wang, B.; Shi, L. *J. Colloid Interface Sci.* **2008**, *322*, 414–420.
(20) Chang, Y.-C.; Chen, D.-H. *J. Hazard. Mater.* **2009**, *165*, 664–669.
(21) Kuroda, K.; Ishida, T.; Haruta, M. *J. Mol. Cat. A: Chem.* **2009**, *298*, 7–11.
(22) Shin, K. S.; Choi, J.-Y.; Park, C. S.; Jang, H. J.; Kim, K. *Catal. Lett.* **2009**, *133*, 1–7.
(23) Arora, S.; Kapoor, P.; Singla, M. L. *React. Kinet. Mech. Catal.* **2010**, *99*, 157–165.
(24) Mahmoud, M. A.; Snyder, B.; El-Sayed, M. A. *J. Phys. Chem. Lett.* **2010**, *1*, 28–31.
(25) Manesh, K. M.; Gopalan, A. I.; Lee, K.-P.; Komathi, S. *Catal. Commun.* **2010**, *11*, 913–918.
(26) Zeng, J.; Zhang, Q.; Chen, J.; Xia, Y. *Nano Lett.* **2010**, *10*, 30–35.
(27) Saha, S.; Pal, A.; Kundu, S.; Basu, S.; Pal, T. *Langmuir* **2010**, *26*, 2885–2893.
(28) Mahmoud, M. A.; Saira, F.; El-Sayed, M. A. *Nano Lett.* **2010**, *10*, 3764–3769.
(29) Sahiner, N.; Ozay, H.; Ozay, O.; Aktas, N. *Appl. Catal., A* **2010**, *385*, 201–207.
(30) Sahiner, N.; Ozay, H.; Ozay, O.; Aktas, N. *Appl. Catal., B* **2010**, *101*, 137–143.
(31) Lu, Y.; Mei, Y.; Walker, R.; Ballauff, M.; Drechsler, M. *Polymer* **2006**, *47*, 4985–4995.
(32) Bhandari, R.; Knecht, M. R. *ACS Catal.* **2011**, *1*, 89–98.
(33) Jiang, H.-L.; Akita, T.; Ishida, T.; Haruta, M.; Xu, Q. *J. Am. Chem. Soc.* **2011**, *133*, 1304–1306.
(34) Mahmoud, M. A.; El-Sayed, M. A. *Nano Lett.* **2011**, *11*, 946–953.
(35) Wunder, S.; Polzer, F.; Lu, Y.; Mei, Y.; Ballauff, M. *J. Phys. Chem. C* **2010**, *114*, 8814–8820.
(36) Schrinner, M.; Polzer, F.; Mei, Y.; Lu, Y.; Haupt, B.; Ballauff, M.; Gödel, A.; Drechsler, M.; Preussner, J.; Glatzel, U. *Macromol. Chem. Phys.* **2007**, *208*, 1542–1547.
(37) Gosh, S. K.; Mandal, M.; Kundu, S.; Nath, S.; Pal, T. *Appl. Catal., A* **2004**, *268*, 61–66.
(38) Gao, Y.; Ding, X.; Zheng, Z.; Cheng, X.; Peng, Y. *Chem. Commun.* **2007**, 3720–3722.
(39) Signori, A. M.; de O. Santos, K.; Eising, R.; Albuquerque, B. L.; Giacomelli, F. C.; Domingos, J. B. *Langmuir* **2010**, *26*, 17772–17779.
(40) Huang, J.; Vongehr, S.; Tang, S.; Lu, H.; Meng, X. *J. Phys. Chem. C* **2010**, *114*, 15005–15010.
(41) Wang, S.; Zhang, M.; Zhang, W. *ACS Catal.* **2011**, *1*, 207–211.
(42) Sarkar, S.; Sinha, A. K.; Pradhan, M.; Basu, M.; Negishi, Y.; Pal, T. *J. Phys. Chem. C* **2011**, *115*, 1659–1673.
(43) Prucek, R.; Kvítek, L.; Panácek, A.; Vancurová, L.; Soukupová, J.; Jancík, D.; Zboril, R. *J. Mater. Chem.* **2009**, *19*, 8463–8469.
(44) Zhou, X.; Xu, W.; Liu, G.; Panda, D.; Chen, P. *J. Am. Chem. Soc.* **2010**, *132*, 138–146.
(45) Somorjai, G. A.; Park, J. Y. *Angew. Chem., Int. Ed.* **2008**, *47*, 9212–9228.
(46) Ertl, G. *Faraday Discuss.* **2002**, *121*, 1–15.
(47) Ballauff, M. *Prog. Polym. Sci.* **2007**, *32*, 1135–1151.
(48) Liu, B. H.; Li, Z. B. *J. Power Sources* **2009**, *187*, 527–534.
(49) Guella, G.; Patton, B.; Miotello, A. *J. Phys. Chem. C* **2007**, *111*, 18744–18750.
(50) Tewari, B. B.; Boodhoo, M. *J. Colloid Interface Sci.* **2005**, *289*, 328–332.
(51) László, K.; Podkoscielny, P.; Daborwski, A. *Langmuir* **2003**, *19*, 5287–5294.
(52) Carregal-Romero, S.; Pèrez-Juste, J.; Hevès, P.; Liz-Marzàn, L. M.; Mulvaney, P. *Langmuir* **2010**, *26*, 1271–1277.
(53) Vannice, M. A. *Kinetics of Catalytic Reactions*; Springer: New York, 2005.
(54) Bielejewska, A.; Bylina, A.; Duszczyk, K.; Fialkowski, M.; Holyst, R. *Anal. Chem.* **2010**, *82*, 5463–5469.
(55) Bond, G. C. *Appl. Catal., A* **2000**, *191*, 23–34.
(56) Bond, G. C.; Kaene, M. A.; Kral, H.; Lercher, J. A. *Catal. Rev. — Sci. Eng.* **2000**, *42*, 323–383.
(57) Rooney, J. J. *J. Mol. Catal. A: Chem.* **1998**, *129*, 131–134.
(58) Bond, G. C. *Catal. Today* **1999**, *49*, 41–48.

(59) Bratlie, K. M.; Li, Y.; Larsson, R.; Somorjai, G. A. *Catal. Lett.* **2008**, *121*, 173–178.
(60) Bligaard, T.; Honkala, K.; Lagodottir, A.; Nørskov, J. K.; Dahl, S.; Jacobsen, J. H. *J. Phys. Chem. B* **2003**, *107*, 9325–9331.
(61) Driver, S. M.; Zhang, T.; King, D. A. *Angew. Chem., Int. Ed.* **2007**, *46*, 700–703.
(62) Baber, A. E.; Jensen, S. C.; Iski, E. V.; Sykes, C. H. *J. Am. Chem. Soc.* **2006**, *128*, 15384–15385.
(63) Hrbek, J.; Hoffmann, F. M.; Park, J. B.; Liu, P.; Stacchiola, D.; Hoo, Y. S.; Ma, S.; Nambu, A.; Rodriguez, J. A.; White, M. G. *J. Am. Chem. Soc.* **2008**, *130*, 17272–17273.
(64) Pierce, M. S.; Chan, K.-C.; Hennessy, D. C.; Komanicky, V.; Menzel, A.; You, H. *J. Phys. Chem. C* **2008**, *112*, 2231–2234.
(65) Hopkinson, A.; Bradley, J. M.; Guo, X.-C.; King, D. A. *Phys. Rev. Lett.* **1993**, *71*, 1597–1600.
(66) van Beurden, P.; Kramer, G. J. *J. Chem. Phys.* **2004**, *121*, 2317–2325.